International Symposium on Information Theory and its Applications, ISITA2006
Seoul, Korea, October 29–November 1, 2006

Influence of Transmit and Receive Correlations on Performance of the MIMO System with Multiple Antennas and Relay Terminals

Ryosuke UCHIDA†, Hiraku OKADA‡, Takaya YAMAZATO†† and Masaaki KATAYAMA††

† Dept. of Electrical Engineering and Computer Science,
Graduate School of Engineering, Nagoya University,
Furo-cho, Chikusa-ku, Nagoya, 464-8603, JAPAN
E-mail: uchida@katayama.nuee.nagoya-u.ac.jp

‡ Center for Transdisciplinary Research, Niigata University,
8050 Nino-cho, Ikarashi, Niigata, 950-2181, JAPAN
E-mail: hiraku@ie.niigata-u.ac.jp

†† EcoTopia Science Institute, Nagoya University,
Furo-cho, Chikusa-ku, Nagoya, 464-8603, JAPAN
E-mail: {yamazato,katayama}@nuee.nagoya-u.ac.jp

Abstract

In this manuscript, spatial diversity for in-factory environments is considered. The proposed scheme uses multiple antennas at a transmitter and a receiver, and also multiple relay terminals to provide diversity gain against fading and shadowing. If the separation of antennas at the transmitter or the receiver is not enough, then diversity gain is influenced by correlation at the transmitter or the receiver. This manuscript shows the analytical and numerical results of the effects of transmit and receive correlations on bit error performance of the proposed spatial diversity scheme.

1. Introduction

Wireless control of industrial machines is a promising application of wireless communications [1, 2, 3]. The wireless transmission of control data is inevitable for moving objects, such as traveling carriages or wheeled robots. Furthermore, freedom from control wires offers the factory layout flexibility of machines.

For the realization of wireless control in factories, communications reliability is essential. One important factor of reliability loss is multipath fading [3, 4]. In factories, radio waves reflected by metal equipment have large amplitudes that cause large attenuation if combined destructively with a direct wave [4]. In addition, the coherent bandwidth of the fading tends to be large compared with the signals, which may have low speed to carry a relatively small amount of control data. As a result, multipath fading attenuates the power of the signal in all its bandwidth and causes the loss of reliable communications.

In addition to multipath fading, the effects of shadowing must be considered, since large metallic machines may interrupt the paths between a transmitter and a receiver.

For both multipath fading and shadowing, we have already proposed a spatial diversity scheme with multiple transmit and receive antennas and relay terminals [5]. Figure 1 illustrates the basic concept of the spatial diversity scheme proposed in [5]. Multiple antennas at a mobile terminal (MT) and a base station (BS) provide diversity gain against fading, while multiple relay terminals (RTs) located in the lines of sight to BS provide diversity gain against shadowing.

It is not difficult to put RTs with large separation between them to ensure independence in shadowing. However, due to the physical size limitations of the MT and BS, it may not be easy to maintain independence of branches to fading with enough large separation of antennas. This is known as transmit and receive correlations [6].

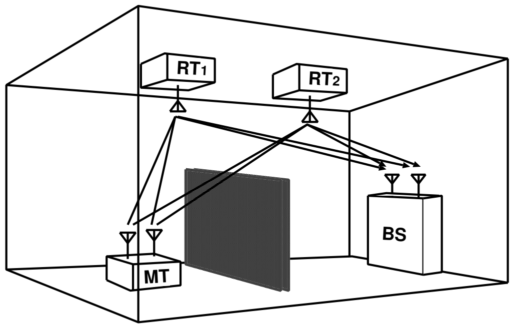

Figure 1: Spatial diversity with multiple-antennas and relay terminals.

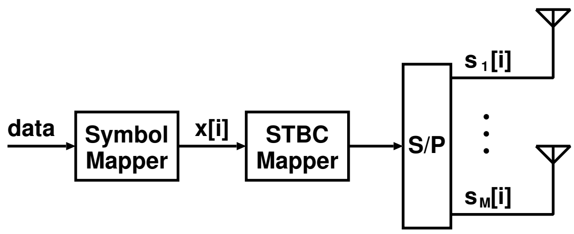

Figure 2: The transmitter.

In this manuscript, the amount of performance degradation due to transmit and receive correlations is analytically derived in a closed form in Sec. 3. Then the results are compared with the results of numerical simulations in Sec. 4.

2. System Model

2.1. Mobile Terminal

This manuscript concentrates on uplink performance. Figure 2 illustrates the equivalent low-pass model of the transmitter at the MT. The input data of $2I$ bits are mapped into the QPSK symbols $\{x[i]\}$ based on Gray encoding as:

$$\{x[1],\cdots,x[i],\cdots,x[I]\}, \tag{1}$$

where I denotes the number of symbols in a frame and

$$x[i] \in \{\exp(\pm j\pi/4), \exp(\pm j3\pi/4)\}. \tag{2}$$

The symbols are then transmitted from the M antennas using the Space-Time Block Code (STBC) [7, 8].

Let the signal transmitted from the m-th transmit antenna in the i-th symbol interval be $s_m[i]$, and then a set of all signals transmitted from the M antennas in the i-th symbol interval is denoted by vector

$$\boldsymbol{s}[i] \;=\; (s_1[i],\cdots,s_M[i])^T, \tag{3}$$

where ^{T} is the transpose of the vector. For example, if $M = 2$,

$$\boldsymbol{s}[i] = \begin{pmatrix} s_1[i] \\ s_2[i] \end{pmatrix} = \begin{cases} \sqrt{\frac{E_s}{2}} \begin{pmatrix} x[i] \\ x[i+1] \end{pmatrix} & (i\text{: even}) \\ \sqrt{\frac{E_s}{2}} \begin{pmatrix} -x^*[i+1] \\ x^*[i] \end{pmatrix} & (i\text{: odd}) \end{cases}, \tag{4}$$

where E_s denotes the total signal energy for the transmission of $\boldsymbol{s}[i]$ from the M transmit antennas.

2.2. Channel between MT and RTs

Signals transmitted from the M antennas, which are influenced by fading and shadowing are received by each RT. Let the number of all RTs be L.

The set of signals received in the i-th symbol interval at all L RTs can be denoted by vector,

$$\boldsymbol{r}_r[i] = \begin{pmatrix} r_{r_1}[i] \\ r_{r_2}[i] \\ \vdots \\ r_{r_L}[i] \end{pmatrix} = \begin{pmatrix} a_{11} & a_{12} & \cdots & a_{1M} \\ a_{21} & a_{22} & \cdots & a_{2M} \\ \vdots & \vdots & \ddots & \vdots \\ a_{L1} & a_{L2} & \cdots & a_{LM} \end{pmatrix} \begin{pmatrix} s_1[i] \\ s_2[i] \\ \vdots \\ s_M[i] \end{pmatrix} + \begin{pmatrix} n_{r_1}[i] \\ n_{r_2}[i] \\ \vdots \\ n_{r_L}[i] \end{pmatrix} \tag{5}$$

$$= \boldsymbol{A}\boldsymbol{s}[i] + \boldsymbol{n}_r[i], \tag{6}$$

where $r_{r_l}[i]$ is the signal received at the l-th RT in the i-th symbol interval and a_{lm} denotes complex channel gain between the l-th RT and the m-th antenna of the MT. The elements of vector $\boldsymbol{n}_r[i]$, $\{n_{r_1}[i], n_{r_2}[i], \cdots, n_{r_L}[i]\}$, denote noise components at the output of each demodulator of RTs and are assumed to be zero mean independently and identically distributed (i.i.d.) complex Gaussian random variables with variance N_0.

Slow Rayleigh fading and log-normal shadowing environments are assumed on the channel between the MT and RTs. On this assumption, a_{lm} becomes a random variable whose instantaneous value changes due to fading and mean-square value changes due to shadowing.

The same shadowing effect is assumed on the channels between the same l-th RT and all M transmit antennas. Then the probability density function of $\mathrm{E}[|a_{lm}|^2] = Z_l$ becomes

$$p_{Z_l}(Z) = \frac{10\log_{10} e}{\sqrt{2\pi}\sigma Z} \exp\left(-\frac{1}{2\sigma^2}\left(10\log_{10} Z + \frac{\ln 10}{20}\sigma^2\right)^2\right), \tag{7}$$

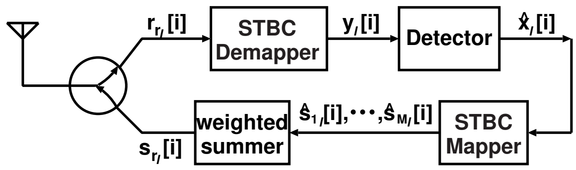

Figure 3: The relay terminal.

where σ denotes the standard deviation of log-normal shadowing [9].

At each RT, fluctuations of signals from the M transmit antennas to the RT due to fading are correlated, but not for different RTs. In this case, for a given Z_l, the correlation matrix of a_{lm} is

$$\mathrm{E}\left[\begin{pmatrix} a_{11} \\ a_{12} \\ \vdots \\ a_{LM} \end{pmatrix} (a_{11}^*, a_{12}^*, \cdots, a_{LM}^*)\right] = \begin{pmatrix} Z_1\boldsymbol{R}_{tx} & \boldsymbol{0} & \cdots & \boldsymbol{0} \\ \boldsymbol{0} & Z_2\boldsymbol{R}_{tx} & \cdots & \boldsymbol{0} \\ \vdots & \vdots & \ddots & \vdots \\ \boldsymbol{0} & \boldsymbol{0} & \cdots & Z_L\boldsymbol{R}_{tx} \end{pmatrix} \tag{8}$$

$$= \mathrm{diag}(Z_1,\cdots,Z_L) \otimes \boldsymbol{R}_{tx}, \tag{9}$$

where $\otimes$ denotes the Kronecker product and $\mathrm{diag}(\cdots)$ denotes a diagonal matrix whose diagonal elements are $\cdots$. Matrix $\boldsymbol{R}_{tx}$ denotes the transmit correlation matrix [10] at MT. In a Rayleigh fading environment, each element of $\boldsymbol{A}$ is a complex Gaussian random variable with mean zero whose correlation matrix is given by Eq. (9).

2.3. Relay Terminals

Figure 3 illustrates the RT that receives signals from the M antennas of the MT and retransmits them to the BS.

The l-th RT estimates the complex gains $\{a_{l1}, a_{l2}, \cdots, a_{lM}\}$. In this study, perfect estimation is assumed. Then received signals $\{r_{r_l}[1], r_{r_l}[2], \cdots, r_{r_l}[i], \cdots\}$ are demapped using the estimates based on STBC into signals $\{y_l[1], y_l[2], \cdots, y_l[i], \cdots, y[I]\}$.

The resulting signal $y_l[i]$ consists of data $x[i]$ and noise terms. For example, if $M = 2$, $y_l[2i]$ and $y_l[2i+1]$ can be written as follows:

$$\begin{pmatrix} y_l[2i] \\ y_l[2i+1] \end{pmatrix} = \begin{pmatrix} a_{l1}^* & a_{l2} \\ a_{l2}^* & -a_{l1} \end{pmatrix} \begin{pmatrix} r_{r_l}[2i] \\ r_{r_l}^*[2i+1] \end{pmatrix} \tag{10}$$

$$= (|a_{l1}|^2 + |a_{l2}|^2) \begin{pmatrix} x[2i] \\ x[2i+1] \end{pmatrix} + \begin{pmatrix} a_{l1}^* n_{r_1}[2i] + a_{l2} n_{r_1}^*[2i+1] \\ a_{l2}^* n_{r_1}[2i] - a_{l1} n_{r_1}^*[2i+1] \end{pmatrix} \tag{11}$$

Signals $\{y_l[1], y_l[2], \cdots, y_l[i], \cdots, y_l[I]\}$ are then processed by the ML detecter to obtain estimates of data symbols $\{\hat{x}_l[1], \hat{x}_l[2], \cdots, \hat{x}_l[i], \cdots, \hat{x}_l[I]\}$. From these $\hat{x}_l[i]$s, estimates of transmitted signals $\hat{\boldsymbol{s}}_l[i] = (\hat{s}_{1_l}[i], \hat{s}_{2_l}[i], \cdots, \hat{s}_{M_l}[i])^T$ are generated by mapping based on STBC. Each RT then retransmits signal $s_{r_l}[i]$, which is obtained by the following equation:

$$s_{r_l}[i] = \alpha(a_{l1}, a_{l2}, \cdots, a_{lM}) \cdot (\hat{s}_{1_l}[i], \hat{s}_{2_l}[i], \cdots, \hat{s}_{M_l}[i])^T, \tag{12}$$

to the BS. In the above equation, α is a constant value.

The set of all signals retransmitted from all L RTs to the BS at the i-th symbol interval can be written by vector

$$\boldsymbol{s}_r[i] \quad = \quad (s_{r_1}[i], s_{r_2}[i], \cdots, s_{r_L}[i])^T. \qquad (13)$$

By employing $\boldsymbol{s}[i]$, Eq. (13) can be rewritten as

$$\boldsymbol{s}_r[i] \quad = \quad \alpha(\boldsymbol{A}\boldsymbol{s}[i] + \boldsymbol{e}_r[i]), \qquad (14)$$

where $\boldsymbol{e}_r[i]$ denotes the errors introduced at the RTs.

Signal $s_{r_l}[i]$ is simultaneously retransmitted from each RT to BS at the same carrier frequency, which is different from that for the channels between MT and RTs.

2.4. Channel between RTs and BS

Signals retransmitted from the L RTs are influenced by fading and received by the BS with N antennas.

The set of signals received in the i-th symbol interval at the BS is given by

$$\begin{pmatrix} r_1[i] \\ r_2[i] \\ \vdots \\ r_N[i] \end{pmatrix} = \begin{pmatrix} b_{11} & b_{12} & \cdots & b_{1L} \\ b_{21} & b_{22} & \cdots & b_{2L} \\ \vdots & \vdots & \ddots & \vdots \\ b_{N1} & b_{N2} & \cdots & b_{NL} \end{pmatrix} \begin{pmatrix} s_{r_1}[i] \\ s_{r_2}[i] \\ \vdots \\ s_{r_L}[i] \end{pmatrix} + \begin{pmatrix} n'_1[i] \\ n'_2[i] \\ \vdots \\ n'_N[i] \end{pmatrix}, \qquad (15)$$

where $r_n[i]$ denotes the received signal at the n-th receive antenna, $n'_n[i]$ denotes the noise sample, which is a complex Gaussian random variable with mean zero and variance N_0, and b_{nl} denotes complex channel gain between the l-th RT and the n-th receive antenna.

Since RTs are placed in the lines of sight to BS, signals transmitted from the RTs arrive at BS without shadowing, but multipath fading may still affect signal strength. At the BS, signals from the same RT are assumed to have correlated fluctuations, while signals from different RTs are assumed to have uncorrelated fluctuations. Thus the correlation matrix of b_{nl}s is given by

$$\mathrm{E}\left[\begin{pmatrix} b_{11} \\ b_{21} \\ \vdots \\ b_{NL} \end{pmatrix} (b^*_{11}, b^*_{21}, \cdots, b^*_{NL})\right] = \begin{pmatrix} \boldsymbol{R}_{rx} & \boldsymbol{0} & \cdots & \boldsymbol{0} \\ \boldsymbol{0} & \boldsymbol{R}_{rx} & \cdots & \boldsymbol{0} \\ \vdots & \vdots & \ddots & \vdots \\ \boldsymbol{0} & \boldsymbol{0} & \cdots & \boldsymbol{R}_{rx} \end{pmatrix} \qquad (16)$$

$$= \boldsymbol{I}_L \otimes \boldsymbol{R}_{rx}, \qquad (17)$$

where $\boldsymbol{I}_L$ denotes $L \times L$ identity matrix and $\boldsymbol{R}_{rx}$ denotes $N \times N$ receive correlation matrix [10].

In the worst case scenario, such as a heavily cluttered LOS [4], fading can be assumed to be Rayleigh, and then channel gains b_{nl}s are multivariate complex Gaussian random variables with mean zero and a covariance matrix given by Eq. (16).

All received signals at N receiving antennas in the i-th symbol interval can also be written by a vector form:

$$\boldsymbol{r}[i] \quad = \quad \boldsymbol{B}\boldsymbol{s}_r[i] + \boldsymbol{n}'[i], \qquad (18)$$

where $\boldsymbol{r}[i]$ is a N dimensional vector that consists of $\{r_n[i]\}$s, $\boldsymbol{B}$ is a $N \times L$ channel matrix which consists of $\{b_{nl}\}$s, and $\boldsymbol{n}'[i]$ is a N dimensional vector which consists of $\{n'_n[i]\}$s.

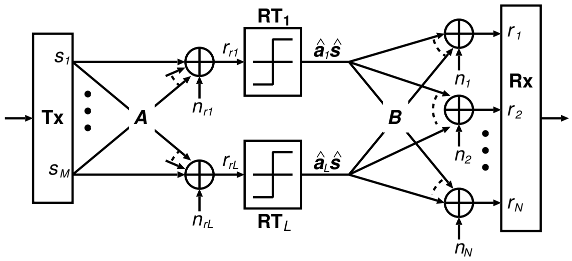

Figure 4: Signal flow between the transmitter and receiver through relay terminals.

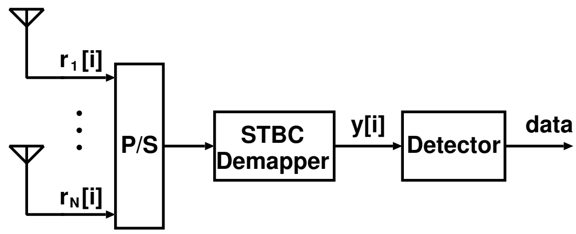

Figure 5: The receiver of the base station.

To summarize the system model, Fig. 4 shows the signal flow diagram from MT to BS. Signals transmitted from MT are received at BS through MIMO channel $\boldsymbol{H} = \boldsymbol{B}\boldsymbol{A}$. By substituting Eq. (14) into Eq. (18), received signals $\boldsymbol{r}[i]$ can be rewritten as

$$\boldsymbol{r}[i] \quad = \quad \alpha\boldsymbol{B}\boldsymbol{A}\boldsymbol{s}[i] + \alpha\boldsymbol{B}\boldsymbol{e}_r[i] + \boldsymbol{n}'[i] \qquad (19)$$

$$= \quad \alpha\boldsymbol{H}\boldsymbol{s}[i] + \boldsymbol{n}[i], \qquad (20)$$

where $\boldsymbol{n}[i] = \boldsymbol{n}'[i] + \alpha\boldsymbol{B}\boldsymbol{e}_r[i]$.

2.5. Base Station

Figure 5 illustrates the BS system model. Received signals $\boldsymbol{r}[i]$ are demapped based on STBC demapper using the estimate of channel matrix $\boldsymbol{H}$, and resulting signals $\{y[1], y[2], \cdots, y[i], \cdots, y[I]\}$ are obtained.

For example, if $M = 2$, the demapped received signals are given by

$$\begin{pmatrix} y[2i] \\ y[2i+1] \end{pmatrix} = \sum_{n=1}^{N} \begin{pmatrix} h^*_{n1} & h_{n2} \\ h^*_{n2} & -h_{n1} \end{pmatrix} \begin{pmatrix} r_n[2i] \\ r^*_n[2i+1] \end{pmatrix}, \quad (21)$$

where h_{nm} denotes the (n,m)-th element of channel matrix $\boldsymbol{H}$.

Based on signals $\{y[1], y[2], \cdots, y[i], \cdots, y[I]\}$, estimates of data symbols $\{\hat{x}[1], \hat{x}[2], \cdots, \hat{x}[i], \cdots, \hat{x}[I]\}$ are obtained by maximum likelihood detection.

3. Effect of Transmit and Receive Correlations on Bit Error Rate

When $L >> M, N$, bit error rate can be approximated by

$$p_e(\gamma|\boldsymbol{A},\boldsymbol{B}) \approx \exp\left(-\frac{\gamma}{2ML}\sum_{n=1}^{N}\sum_{l=1}^{L}\lambda_l|\beta_{nl}|^2\right), \quad (22)$$

where γ denotes the average signal to noise ratio (SNR) for each receive antenna [11]. The value of γ contains both the error introduced at RTs and the noise at BS. In the equation, $\{\lambda_1, \lambda_2, \cdots, \lambda_L\}$ are L eigenvalues of matrix

$$\boldsymbol{C} = \boldsymbol{A}\boldsymbol{A}^H, \quad (23)$$

and β_{nl} is obtained by

$$(\beta_{n1}, \beta_{n2}, \cdots, \beta_{nL})^T = \boldsymbol{U}^H(b_{n1}, b_{n2}, \cdots, b_{nL})^T, \quad (24)$$

where $\boldsymbol{U}$ is a unitary matrix that satisfies the following equation:

$$\boldsymbol{C} = \boldsymbol{U}\boldsymbol{\Lambda}\boldsymbol{U}^H. \quad (25)$$

Now let us average bit error probability, given by Eq. (22), over the distribution of $\boldsymbol{B}$. Since elements $\{b_{nl}\}$ of channel matrix $\boldsymbol{B}$ are transformed by Eq. (24) into $\{\beta_{nl}\}$ on the right side of Eq. (22), the probability distribution of $\{\beta_{nl}\}$ should be derived from the probability distribution of $\{b_{nl}\}$.

Elements $\{b_{nl}\}$ of channel matrix $\boldsymbol{B}$ are multivariate complex Gaussian random variables with mean zero and covariance matrix given by Eq. (16). Thus from Eq. (24), $\{\beta_{nl}\}$ are also multivariate complex Gaussian random variables with mean zero and covariance matrix $\boldsymbol{P}_\beta$, where $\boldsymbol{P}_\beta$ is a $NL \times NL$ matrix given by [12]

$$\begin{aligned}\boldsymbol{P}_\beta &= \mathrm{E}\left[\begin{pmatrix}\beta_{11}\\ \beta_{21}\\ \vdots\\ \beta_{NL}\end{pmatrix}(\beta_{11}^*, \beta_{21}^*, \cdots, \beta_{NL}^*)\right].\\ &= \mathrm{E}\left[\boldsymbol{U}^H \otimes \boldsymbol{I}_N \begin{pmatrix}b_{11}\\ b_{21}\\ \vdots\\ b_{NL}\end{pmatrix}(b_{11}^*, b_{21}^*, \cdots, b_{NL}^*)\boldsymbol{U} \otimes \boldsymbol{I}_N\right].\\ &= (\boldsymbol{U}^H \otimes \boldsymbol{I}_N)(\boldsymbol{I}_L \otimes \boldsymbol{R}_{rx})(\boldsymbol{U} \otimes \boldsymbol{I}_N).\\ &= \boldsymbol{I}_L \otimes \boldsymbol{R}_{rx}. \end{aligned} \quad (26)$$

The covariance matrix given by the above equation is exactly identical to that given by Eq. (16). This fact means that the correlation matrix is invariant under transformation by unitary matrix $\boldsymbol{U}$.

For simple notation, let us define NL dimensional vector:

$$\boldsymbol{\beta} = (\beta_{11}, \beta_{21}, \cdots, \beta_{N1}, \beta_{12}, \cdots, \beta_{N2}, \cdots, \beta_{1L}, \cdots, \beta_{NL}.) \quad (27)$$

Then the joint probability density function of $\boldsymbol{\beta}$ is given by

$$p(\boldsymbol{\beta}) = \frac{1}{(2\pi)^{NL}(\det\boldsymbol{P}_\beta)}\exp\left(-\frac{1}{2}\boldsymbol{\beta}^H\boldsymbol{P}_\beta^{-1}\boldsymbol{\beta}\right). \quad (28)$$

By employing the joint probability density function of $\boldsymbol{\beta}$, given by Eq. (28), Eq. (22) can be averaged as

$$\begin{aligned}\overline{p_e(\gamma|\boldsymbol{A})} &\approx \int_{\boldsymbol{\beta}}\exp\left(-\frac{\gamma}{2ML}\sum_{n=1}^{N}\sum_{l=1}^{L}\lambda_l|\beta_{nl}|^2\right)p(\boldsymbol{\beta})d\boldsymbol{\beta}\\ &= \frac{1}{\det\left(\frac{\gamma}{ML}\mathrm{diag}(\lambda_1, \cdots, \lambda_L) \otimes \boldsymbol{R}_{rx} + \boldsymbol{I}_{NL}\right)}.\end{aligned} \quad (29)$$

In Eq. (29), if $L >> M$, the rank of matrix $\boldsymbol{C}$ becomes M and thus

$$\lambda_{M+1} = \lambda_{M+2} = \cdots = \lambda_L = 0. \quad (30)$$

If γ is large,

$$\frac{\gamma}{ML}\lambda_l >> 1, \qquad \forall l \in [0, M], \quad (31)$$

and the denominator of Eq. (29) can be approximated as

$$\det\left(\frac{\gamma}{ML}\mathrm{diag}(\lambda_1, \cdots, \lambda_M) \otimes \boldsymbol{R}_{rx}\right). \quad (32)$$

With this approximation, Eq. (29) can be rewritten as

$$\overline{p_e(\gamma|\boldsymbol{A})} \approx \left(\frac{\gamma}{ML}\right)^{-MN}\frac{1}{(\det(\mathrm{diag}(\lambda_1, \cdots, \lambda_M)))^N(\det\boldsymbol{R}_{rx})^M}. \quad (33)$$

Let us next consider the average of Eq. (33) over the probability distribution of $\boldsymbol{A}$. First, $\boldsymbol{A}$ can be transformed into $\boldsymbol{A}'$ as

$$\boldsymbol{A}' = \boldsymbol{A}\boldsymbol{R}_{tx}^{-1/2}. \quad (34)$$

Then each element of $\boldsymbol{A}'$ is mutually uncorrelated. Eq. (33) can be rewritten by using $\boldsymbol{A}'$ as

$$\overline{p_e(\gamma|\boldsymbol{A}')} \approx \left((\det\boldsymbol{R}_{tx})^{\frac{1}{M}}(\det\boldsymbol{R}_{rx})^{\frac{1}{N}}\frac{\gamma}{ML}\right)^{-MN}\frac{1}{\left(\det\boldsymbol{A}'^H\boldsymbol{A}'\right)^N}. \quad (35)$$

In the above equation, probability distribution of $\boldsymbol{A}'^H\boldsymbol{A}'$ becomes the product of Wishart [13] and log-normal distributions, which complicates averaging Eq. (35). However, the amount of SNR degradation due to transmit and receive correlations can be given by Eq. (35). In this equation, each element of $\boldsymbol{A}'$ is uncorrelated, and thus it does not contain any effects of transmit or receive correlations. Hence even if $\overline{p_e(\gamma|\boldsymbol{A}')}$ is not averaged over the probability distribution of $\boldsymbol{A}'$, SNR degradation due to transmit and receive correlations can be given as

$$(\det\boldsymbol{R}_{tx})^{\frac{1}{M}}(\det\boldsymbol{R}_{rx})^{\frac{1}{N}}. \quad (36)$$

4. Numerical Examples

4.1. Parameters for Simulations

In simulations for numerical examples, the standard deviation of log-normal shadowing σ is assumed to be 8 [dB], which is a moderate value in factory environments [4].

Both the numbers of antennas at MT (M) and BS (N) are assumed to be two, and their transmit and receive correlations matrices have form

$$\boldsymbol{R}_{tx} = \begin{pmatrix} 1 & c_{tx} \\ c_{tx}^* & 1 \end{pmatrix}, \quad (37)$$

and

$$\boldsymbol{R}_{rx} = \begin{pmatrix} 1 & c_{rx} \\ c_{rx}^* & 1 \end{pmatrix}, \quad (38)$$

respectively [10].

For simplicity of discussion, all distances, or average propagation losses, between MT and RT are assumed to be the same, and the same assumption is applied between RTs and BS. It is also assumed that $\alpha = 1/L$. Under these assumptions,

$$\overline{\left(\frac{|\boldsymbol{a}_l \cdot \boldsymbol{s}[i]|^2}{|n_{r_l}[i]|^2}\right)} = \overline{\left(\frac{|\boldsymbol{b}_n \cdot \boldsymbol{s}_r[i]|^2}{|n'_n[i]|^2}\right)} = \overline{\gamma}, \quad {}^\forall l, n. \quad (39)$$

In this equation, $\boldsymbol{a}_l$ is the l-th row vector of $\boldsymbol{A}$ given in Eq. (6), and $\boldsymbol{b}_n$ denotes the n-th row vector of $\boldsymbol{B}$ given in Eq. (18).

4.2. Average Bit Error Rate

Figure 6 shows average bit error rate as a function of SNR given in Eq. (39). In this figure, moderate correlation ($c_{tx} = 0.75 + j0.08$) is assumed at the transmitter (MT) and light correlation ($c_{rx} = 0.30$) is assumed at the receiver (BS) [14]. For comparison, performance without antenna correlation $c_{tx} = c_{rx} = 0$ is also shown.

The figure also shows performance degradation caused by transmit/receive correlation. An increase of L (the number of RTs) provides performance improvement. Under the presence of antenna correlations, diversity gains at $\overline{\mathrm{BER}} = 10^{-3}$ compared to $L = 2$ are 4 [dB] with $L = 3$ and 8 [dB] with $L = 5$.

From the figure, performance with correlation is inferior to performance without correlation (non-correlative). The amount of performance degradation at $\overline{\mathrm{BER}} = 10^{-3}$ is always about 1 to 2 [dB] for various values of L including an extreme case, i.e., $L = 20$. In other words, the degree of performance degradation caused by transmit and receive correlations is not sensitive to the number of RTs. This fact implies that performance degradation due to correlations can be compensated for by increasing the number of RTs.

Note that the amount of performance degradation 1–2 [dB] agrees with the result of Eq. (36), which suggests that the amount of performance degradation is $(\det \boldsymbol{R}_{tx} \det \boldsymbol{R}_{rx})^{\frac{1}{2}} = -2.07$ [dB].

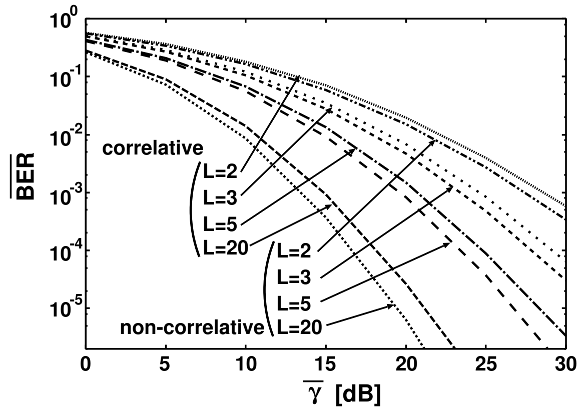

Figure 6: Average bit error rate in a shadowing environment.

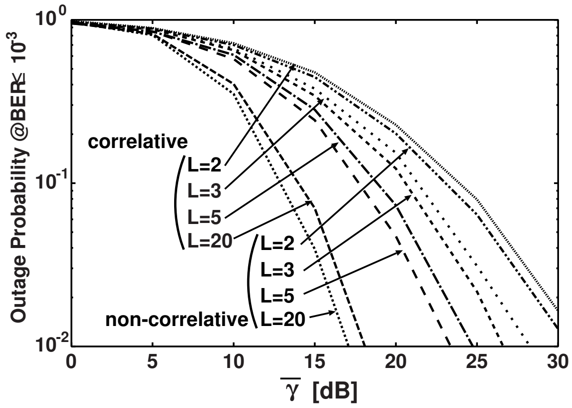

Figure 7: Outage Probability that the bit error rate exceeds 10^{-3}.

4.3. Outage Probability of Bit Error Rate

The outage probability that the bit error rate exceeds 10^{-3} as a function of SNR in Fig. 7 also shows similar characteristics to average bit error rate. Outage probability also decreases due to transmit and receive correlations. Note that the amount of performance degradation is about 1 [dB], which also agrees with the result of Eq. (36).

4.4. Comparison of Theoretical and Numerical Results with Various Correlation Matrices

In the above subsections, numerical examples are shown for a set of relatively light correlations. To discuss the effects of correlations, two additional cases [10] are considered in this subsection.

Table 1 shows the degree of performance degradation caused by correlations, measured by the required average SNR at $\overline{\mathrm{BER}}$ 10^{-5}. In the table, ① is the light correlation case discussed in the previous subsections. The moderately correlating case is ②, and ③ provides heavy correlations.

The numerical examples in the table shows that large

Table 1: Performance degradation at $\overline{\text{BER}} = 10^{-5}$.

	c_{tx}	c_{rx}	by Eq.(36)	by Simulation ($L = 5$)	by Simulation ($L = 20$)
①	0.75+j0.08	0.30	-2.07 [dB]	-1.68 [dB]	-1.80 [dB]
②	-0.12-j0.18	-0.61+j0.77	-7.38 [dB]	-4.36 [dB]	-5.36 [dB]
③	-0.61+j0.77	-0.61+j0.77	-14.6 [dB]	-9.40 [dB]	-10.3 [dB]

correlations result in large degradations. It is also shown that for all three cases, the degree of performance degradation is insensitive to the number of RTs.

The examples in the table also show that the results given by Eq. (36) overestimate performance degradation, particularly in large correlation cases such as ③. One reason for this overestimation is the approximation given by Eq. (32). If the correlation is high, then the non-diagonal elements of $\boldsymbol{R}_{rx}$ become large, and Eq. (32) becomes much smaller than the denominator of Eq. (29). Thus the amount of degradation is overestimated.

5. Conclusion

In this manuscript, performance of an MIMO diversity scheme with relay terminals in the presence of transmit and receive correlations was analyzed and evaluated. From analytical and numerical evaluations, the amount of performance degradation was given as a function of transmit and receive correlations. It is also shown that performance degradation due to the correlations can be compensated for by increasing the number of RTs.

Acknowledgments

This work is partly supported by the 21st Century COE Program by the Ministry of Education, Culture, Sports, Science and Technology in Japan.

References

[1] F.L. Lian, J. Moyne, and D. Tilbury, "Network design consideration for distributed control systems," IEEE Transaction on Control Systems Technology, vol.10, no.2, pp.297–307, March 2002.

[2] N.J. Ploplys, P.A. Kawka, and A.G. Alleyne, "Closed-loop control over wireless networks," IEEE Control Systems Magazine, vol.24, no.3, pp.58–71, June 2004.

[3] A. Willig, K. Matheus, and A. Wolisz, "Wireless technology in industrial networks," Proceedings of the IEEE, vol.93, no.6, pp.1130–1151, June 2005.

[4] T.S. Rappaport, "Indoor radio communications for factories of the future," IEEE Communicationis Magazine, vol.27, pp.15–24, May 1989.

[5] R. Uchida, H. Okada, T. Yamazato, and M. Katayama, "A mimo system with relay terminals for reliable wireless control," Proc. of The 16th Annual IEEE International Symposium on Personal, Indoor and Mobile Radio Communication, September 2005.

[6] R.B. Ertel, P. Cardieri, K.W. Sowerby, T.S. Rappaport, and J.H. Reed, "Overview of spatial channel models for antenna array communication systems," IEEE Personal Communicationis, vol.5, no.1, pp.10–22, February 1998.

[7] S.M. Alamouti, "A simple transmit diversity technique for wireless communications," IEEE Journal on Selected Areas in Communications, vol.16, no.8, pp.1451–1458, March 1998.

[8] V. Tarokh, H. Jafarkhani, and A.R. Calderbank, "Space-time block codes from orthogonal designs," IEEE Transaction on Information Theory, vol.45, no.5, pp.1456–1467, July 1999.

[9] R. Uchida, H. Okada, T. Yamazato, and M. Katayama, "Outage probability of a macro and micro mimo diversity scheme in an indoor fading and shadowing environment," IEICE Transaction on Fundamentals of Electronics, Communications and Computer Sciences, vol.E88-A, no.10, pp.2945–2951, October 2005.

[10] J.P. Kermoal, L. Schumacher, K. Ingemann, P.E. Mogensen, and F. Frederiksen, "A statistical mimo radio channel model with experimental validation," IEEE Journal on Selected Areas in Communications, vol.20, no.6, pp.1211–1226, August 2002.

[11] R. Uchida, H. Okada, T. Yamazato, and M. Katayama, "A macro and micro diversity scheme with relay terminals for reliable wireless control," Technical Report of IEICE RCS2005-28, IEICE, June 2005.

[12] R.A. Horn, and C.R. Johnson, Topics in Matrix Analysis, Cambridge University Press, 1991.

[13] A.M. Kshirsagar, Multivariate Analysis, Marcel Dekker, Inc., 1972.

[14] M. Juntti, M. Vehkapera, J. Leinonen, Z. Li, D. Tujkovic, S. Tsumura, and S. Hara, "Mimo mc-cdma communications for future cellular systems," IEEE Communicationis Magazine, vol.43, pp.118–124, February 2005.